



Chrysin Protects Against Titanium Particle-Induced Osteolysis by Attenuating Osteoclast Formation and Function by Inhibiting NF- κ B and MAPK Signaling

OPEN ACCESS

Edited by:

Ning Zhang,
Stanford University, United States

Reviewed by:

Hirohito Hirata,
Stanford University, United States
Bin Wang,
Guangzhou Regenerative Medicine
and Health Guangdong Laboratory,
China

*Correspondence:

Ren Xu
xuren526@xmu.edu.cn
Xin Xu
dr_xuxin2021@163.com
Feng Xu
xufenghou@163.com

[†]These authors have contributed
equally to this work

Specialty section:

This article was submitted to
Integrative and Regenerative
Pharmacology,
a section of the journal
Frontiers in Pharmacology

Received: 11 October 2021

Accepted: 25 January 2022

Published: 23 March 2022

Citation:

Wu Z, Li C, Chen Y, Liu Q, Li N, He X,
Li W, Shen R, Li L, Wei C, Shao S, Fu F,
Ding J, Sun X, Wang D, Yuan G, Su Y,
Zhao J, Xu J, Xu R, Xu X and Xu F
(2022) Chrysin Protects Against
Titanium Particle-Induced Osteolysis
by Attenuating Osteoclast Formation
and Function by Inhibiting NF- κ B and
MAPK Signaling.
Front. Pharmacol. 13:793087.
doi: 10.3389/fphar.2022.793087

Zuoxing Wu^{1,2†}, Chen Li^{1†}, Yu Chen^{2†}, Qian Liu¹, Na Li², Xuemei He², Weibin Li³, Rong Shen², Li Li⁴, Chenming Wei¹, Siyuan Shao¹, Fangsheng Fu¹, Jiaxin Ding¹, Xiaochen Sun¹, Dairong Wang⁵, Guixin Yuan⁶, Yiji Su¹, Jinmin Zhao¹, Jiake Xu⁷, Ren Xu^{1,2,8*}, Xin Xu^{1*} and Feng Xu^{1,9*}

¹Research Centre for Regenerative Medicine, Guangxi Key Laboratory of Regenerative Medicine, Guangxi Medical University, Nanning, China, ²Fujian Provincial Key Laboratory of Organ and Tissue Regeneration, School of Medicine, Xiamen University, Xiamen, China, ³Xiang'an Hospital, School of Medicine, Xiamen University, Xiamen, China, ⁴Pharmaceutical College, Guangxi Medical University, Nanning, China, ⁵Department of Orthopedics, Guilin People's Hospital, Guilin, China, ⁶Department of Orthopedics, The Second Affiliated Hospital, Shantou University Medical College, Shantou, China, ⁷School of Biomedical Sciences, The University of Western Australia, Perth, WA, Australia, ⁸Department of Orthopedic Surgery, The First Affiliated Hospital of Xiamen University, Xiamen, China, ⁹Department of Subject Planning, Ninth Peoples Hospital Shanghai, Jiaotong University School of Medicine, Shanghai, China

Bone homeostasis only exists when the physical function of osteoblast and osteoclast stays in the balance between bone formation and resorption. Bone resorption occurs when the two processes are uncoupled, shifting the balance in favour of bone resorption. Excessive activation of osteoclasts leads to a range of osteolytic bone diseases including osteoporosis, aseptic prosthesis loosening, rheumatoid arthritis, and osteoarthritis. Receptor activator of nuclear factor κ -B ligand (RANKL) and its downstream signaling pathways are recognized as key mediators that drive the formation and activation of osteoclastic function. Hence, osteoclast formation and/or its function remain as dominant targets for research and development of agents reaching the treatment towards osteolytic diseases. Chrysin (CHR) is a flavonoid with a wide range of anti-inflammatory and anti-tumor effects. However, its effect on osteoclasts remains unknown. In this study, we found the effects of CHR on inhibiting osteoclast differentiation which were assessed in terms of the number and size of TRAcP positive multinucleated osteoclasts (OCs). Further, the inhibitory effects of CHR on bone resorption and osteoclast fusion of pre-OC were assessed by hydroxyapatite resorption pit assay and F-actin belts staining; respectively. Western blotting analysis of RANKL-induced signaling pathways and immunofluorescence analysis for p65 nuclear translocation in response to RANKL-induced osteoclasts were used to analyze the mechanism of action of CHR affecting osteoclasts. Lastly, the murine calvarial osteolysis model revealed that CHR could protect against particle-induced bone destruction *in vivo*. Collectively, our data strongly suggested that CHR with its promising anti-tumor effects would also be a potential therapeutic agent for osteolytic diseases.

Keywords: osteoclast, chrysin, osteolysis, NF- κ B, MAPK

INTRODUCTION

The dynamical homeostasis of bone is coordinated by two individual but inter-coupling processes, osteoclast (OC)-mediated bone resorption and osteoblast-mediated bone formation (Boyle et al., 2003; Kular et al., 2012). Excessive OC bone resorption is associated with many osteolytic diseases, including osteoporosis, aseptic prosthetic loosening, rheumatoid arthritis, and periodontitis (Hadjidakis and Androulakis, 2006; Kim et al., 2013). Total joint replacement (TJA) is a common orthopaedic surgery. The purpose of this surgery is to alleviate joint pain associated with end-stage joint diseases (such as osteoarthritis and osteoporotic fractures), restore joint flexibility, and improve the quality of life of patients. However, aseptic prosthesis loosening caused by inflammatory local osteolysis has always been a common complication of TJA. Complication of aseptic prosthetic loosening resulted in poor life quality of patients when long-time wearing become abrasive and painful (Wooley and Schwarz, 2004; Yunpeng et al., 2013). Traced to its cause, long-term complications of TJA were mainly caused by the aseptic prosthesis loosening by common particle-derived prosthetic materials, including ultra-high molecular weight polyethylene (UHMWPE) and metal biomaterial implants. Although the specific mechanism of prosthetic loosening remains unclear, it is believed that the abrasive wear particles induce local cells to release chemokines and cytokines that activate OC formation resulting in the increase of bone resorption and bone loss around the prosthesis (Anderson et al., 2008).

Macrophage colony-stimulating factor (M-CSF) and receptor activator of nuclear factor- κ B ligand (RANKL) have been regarded as the two key cytokines for OC formation (Lacey et al., 1998; Teitelbaum, 2000). M-CSF bridged the RANKL-mediated OC precursor fusion through promoting OC precursor proliferation and survival, and increasing RANK expression (Arai et al., 1999). RANKL belongs to the tumor necrosis factor (TNF) superfamily due to its similar molecular structure and bio-function (Thaler et al., 2016). Various downstream signaling pathways such as NF- κ B and MAPKs (p38, JNK1/2, and ERK1/2) received the activation signals from adaptor proteins TNF receptor-associated factors (TRAFs), in particular TRAF6, which being recruited after RANKL binds to its cognate receptor RANK. This leads to the activation of transcription factors in the nucleus c-Fos and NFATc1 to induce the expression of OC-specific genes such as tartrate resistant acid phosphatase (*Acp5*), V-ATPase V0 domain subunit d2 (*Atp6v0d2*), calcitonin receptor (*Ctr*), and matrix metalloproteinase-9 (*Mmp-9*) (Matsuo et al., 2004; Nakashima and Takayanagi, 2015). Therefore, agents that can restrain the differentiation and/or bone resorption function of OCs are prime drug candidates for the protection of local osteolysis disease.

In recent years, natural compounds have demonstrated many beneficial biological effects including anti-oxidative and anti-inflammatory effects, wherein many of them show therapeutic potential in the treatment of a variety of disease conditions such as bone metabolic disorders

(Norman, 2002; Wang et al., 2017). For example, the Chinese medicine alkaloid, bulleyaconitine A (BLA) and its analogues, being approved for the treatment of chronic pain and rheumatoid arthritis, are likely to be candidate compounds for treating osteoporosis and osteolytic conditions. BLA takes action in inhibiting OC function and promoting bone mineralization by stimulating osteoblasts (Zhang et al., 2018). With natural compounds being in abundance, novel candidates with therapeutic potency could be developed to protect bone destruction from OC over-activation and to provide new medical options to osteolytic bone diseases. Chrysin (CHR) is a natural flavonoid found in honey and propolis, fruits, vegetables, and certain beverages at low concentrations. It shows a variety of potential clinical applications, and has been reported to exhibit anti-inflammatory (Funakoshitago et al., 2016; Nile et al., 2017), anti-oxidative (Zeinali et al., 2017; Wu et al., 2018), and anti-tumorigenic (Nagasaka et al., 2018; Wang et al., 2018) effects. Furthermore, the inflammation caused by LPS induction could be blocked by CHR through attenuating JNK and NF- κ B signaling cascades (Ha et al., 2010), thereby providing a compelling basis for exploring its effects on osteoclastogenesis and bone resorption.

Chrysin (CHR) is a flavonoid compound with a variety of anti-inflammatory and anti-tumor effects. However, the effects of CHR on osteoclasts and LPS-induced inflammatory osteolysis remain unclear. In this study, we aimed to determine the effects of CHR on OC formation and function *in vitro*, and on abrasive osteolysis *in vivo*, and to define the molecular mechanisms by which CHR exerts these effects. The results of this study aim to provide a theoretical basis for the clinical application of CHR in the treatment of osteolysis.

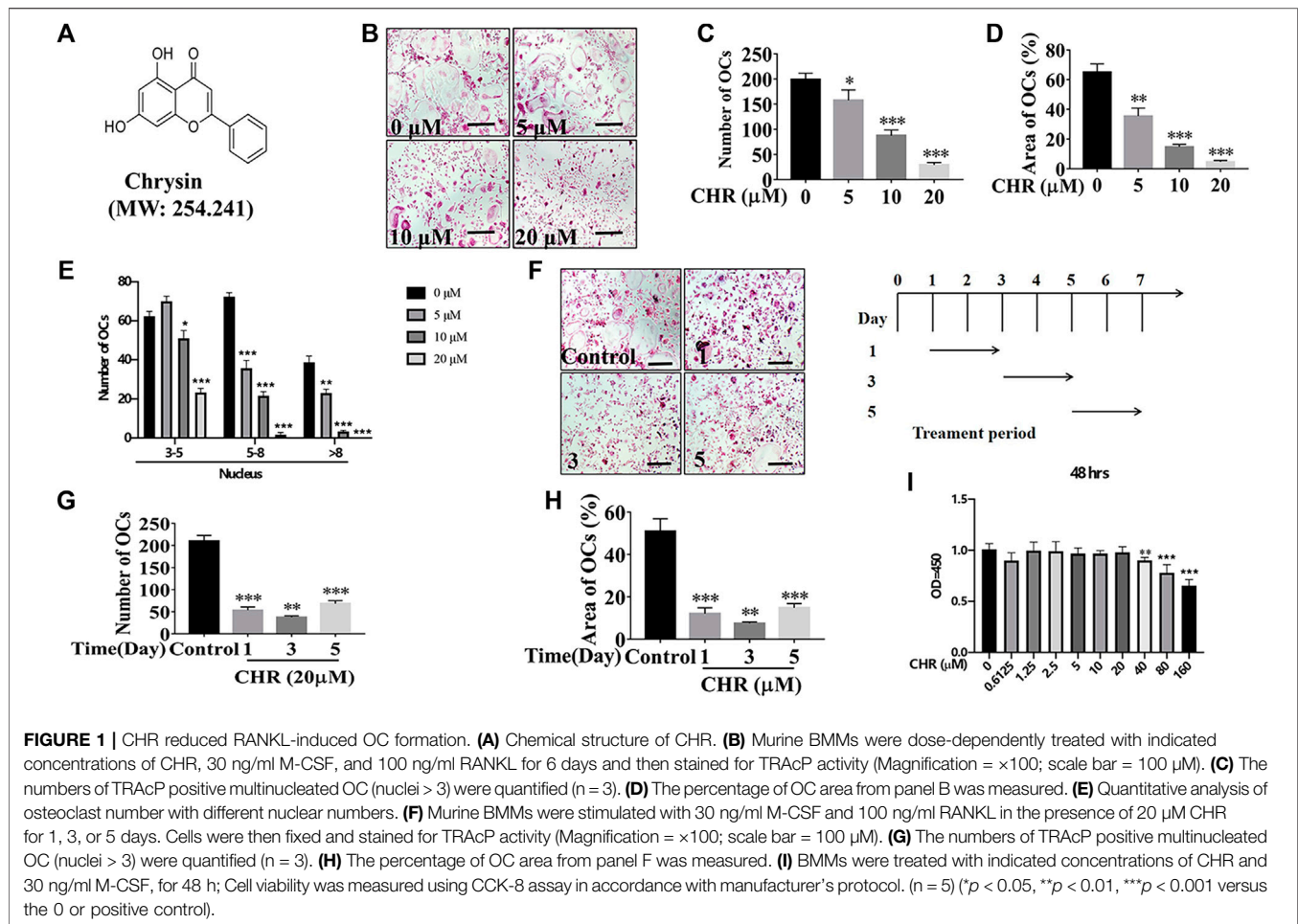
MATERIALS AND METHODS

Reagents

Chrysin (purity > 98% **Figure 1A**) was purchased from Aladdin reagent co., LTD (Shanghai, China). Recombinant mice M-CSF was obtained from R&D Systems (Minneapolis, MN, United States). The purification process of Recombinant RANKL followed the protocol as previously reported (Xu et al., 2000). The CCK8 assay kits were purchased from Promega (Madison, WI, United States). Antibodies for ERK, phospho-ERK, I κ B α , phospho-I κ B α , and β -Actin were obtained from Abcam (Cambridge, United Kingdom). Anti-phospho-JNK, anti-JNK, anti-phospho-p38, anti-p38, anti-phospho-NF- κ B p65, and anti-NF- κ B p65 were obtained from Cell Signaling Technology (Boston, United States).

Cell Culture and Cell Viability Assay

The first step was to obtain murine bone marrow monocyte/macrophages (BMMs) that were isolated from 6 to 8 weeks old male C57BL/6 mice weighing about 20 g. Complete medium of a-MEM with supplement of 10% (v/v) FBS 1% (w/v) penicillin/



streptomycin, and 30 ng/ml M-CSF was used for cell growth in a humidified incubator at 37°C and 5% CO₂ cultured until ready for further applications. To assess the cytotoxic effects of CHR on BMMs, cell viability was determined using the CCK8 cytotoxicity assay. BMMs were seeded at a density of 8×10^3 cells/well in 96-well plates and cultured with M-CSF (30 ng/ml) in the absence or presence of CHR (0.625–160 μM) for 48 and 96 h. CCK8 solution (10 μl /well) was added to each well and incubated with cells for 1.5 h. The absorbance at 450 nm was detected by microplate reader (Thermo, United States).

Osteoclast Formation Assay *In Vitro*

The observation of whether OC differentiation was inhibited under the CHR administration was conducted by tartrate resistant acid phosphatase (TRAcP) activity staining. M-CSF-dependent BMMs were seeded into 96-well plates as 8×10^3 cells/well with complete α -MEM. Cells were placed overnight ensuring the tight adhesion. Stimulation of BMMs using 100 ng/ml RANKL combined with gradually doubling of CHR (from 5, 10 to 20 μM , dose-dependent effect) in every other day. Replacement of culture media containing M-CSF, RANKL, and CHR occurred every 2 days to generate mature multinucleated OCs. Cells were fixed with 4% paraformaldehyde

TABLE 1 | The primer sets used are as follows.

DC-STAMP	Forward: 5'-CTTGCAACCTAAGGGCAAAG-3' Reverse: 5'-TCAACAGCTCTGTCTGTA CC-3'
ACP5	Forward: 5'-TGTGGCCATCTTTATGCT-3' Reverse: 5'-GTCATTTCTTTGGGGCTT-3'
CTR	Forward: 5'-TGCAGACAACCTTTGGTTGG Reverse: 5'-TCGGTTTCTTCTCCTCTGGA
ATP6V0d2	Forward: 5'-GTGAGACCTTGAAGACCTGAA-3' Reverse: 5'-GAGAAATGTGCTCAGGGGCT-3'
MMP-9	Forward: 5'-CGTGTCTGGAGATTCGACTTGA-3' Reverse: 5'-TTGGAACCTCACACGCCAGA-3'
β -actin	Forward: 5'-TCTGCTGGAAGGTGGACAGT-3' Reverse: 5'-CCTCTATGCCAACACAGTGC-3'
CTSK	Forward: 5'-GGCCAACCTCAAGAAGAAAAC3' Reverse: 5'-GTGCTTGTCTCCCTTCTGG-3'

for 15–20 min, followed by the staining of TRAcP activity. Scoring criteria obeyed the rule that the number of TRAcP-positive cells with more than 3 nuclei would be counted as mature osteoclasts.

Real-Time PCR Analysis

Real-time PCR was used for investigating the expression of specific OC genes at the end of OC formation after the application of CHR. The cell RNA extraction reagents and conditions for the real-time

PCR instrumentation were as previously described (Masanori et al., 2010). **Table 1** shows the related primer sets.

Resorption Pit Assay

BMMs were initially seeded into 6-well plates at a density of 1×10^5 cells/well under the cultivation of additional 100 ng/ml RANKL and the small osteoclastic cells appeared at the third or fourth day. On day 4, cells were transferred to hydroxyapatite-coated 96-well plates (Corning, United States) and treated with 10 or 20 μ M CHR and maintained for an additional 2 days. The mature OCs were removed using 10% sodium hypochlorite for 15 min after osteoclast formation was observed, washed twice with PBS, and dried. Light microscopic images captured for each well and pit area were quantified by ImageJ.

F-Actin Ring Staining

BMMs were seeded with 8×10^3 cells/well into 96-well plates and cultured in complete α -MEM medium containing M-CSF (30 ng/ml), RANKL (100 ng/ml), and CHR (10 and 20 μ M) respectively, ensuring the formation of mature multinucleated OC. On day 6 cells were fixed with 4% paraformaldehyde and then were washed, followed by permeabilization under the condition of 0.1% Triton X-100 with 100 μ l volume in each well for 5 min. The 3% BSA in PBS was used to block with Non-specific immuno-reactivity. Cells were washed and incubated with Rhodamine-conjugated phalloidin for 1–2 h to stain actin. Following washes 3 times with PBS, cells were counterstained with DAPI for 5 min. Then the fluorescence microscope was used for obtaining images.

Western Blot Analysis

BMMs were seeded in 6-well plates and maintained until >90% confluence. Cells were serum-starved for 2 h. The treatment group was treated with 20 μ M CHR for 2 h, subsequent by stimulation with RANKL at a concentration of 100 ng/ml in time points (discarding RANKL at 5, 10, 20, 30, or 60 min). To explore the effect of Chrysin on RANKL-induced osteoclast signaling events, nuclear and cytoplasmic proteins were extracted from BMMs after combination of stimulation presence or absence 20 μ M CHR for 1, 3, or 5 days together with RANKL. Untreated cells served as control. Total cellular protein from each sample was extracted using RIPA buffer contained with PMSF and phosphatase inhibitor. Next, 20 μ g of total cellular protein lysate transfected with nitrocellulose membrane by 10% SDS-PAGE. Subsequently, the 5% BSA in TBST (50 mM Tris, pH 7.6; 150 mM NaCl; and 0.1% Tween-20) were used incubated with membrane for one and a half hours and incubated with primary antibody (1:1000) for 12–15 h at 4°C. Subsequently, the membranes were washed 3 times with TBST, and incubated with the IRDye fluorescent secondary antibody corresponding to the primary antibody for 1 h at room temperature. The immuno-reactive bands were analyzed using The Odyssey Infrared Imaging System (LI-COR).

Titanium Particle-Induced Murine Calvarial Osteolysis Model *In Vivo*

A total of healthy 24 male C57BL/6 mice were obtained from Guangxi Medical University's Animal Experiment Center and were randomly assigned into 4 experimental groups wherein each

group included 6 mice: Sham group, vehicle group, low-dose CHR group, and high-dose CHR group. After anesthesia with 10% chloral hydrate in the abdomen, 30 mg of titanium particles were embedded under the periosteum located at the middle suture of the mouse skull. No particles were embedded in the Sham group. CHR was injected into the calvaria of mice every other day at 4 (low dose) or 8 mg/kg (high dose) for 14 days. Sham and vehicle groups received same volume PBS injections every 2 days during the 14 days of the experimental period. At the end of the experiment, all experimental mice were sacrificed, calvariae were isolated and fixed in 4% paraformaldehyde for subsequent micro-CT scanning, and histological sectioning as previously reported (Qin et al., 2012).

Micro-CT, Histology, and Histomorphometric Analysis

The scanned images of whole calvarial were reconstructed and analyzed for the degree of calvarial osteolysis using high-resolution Microcomputed tomography (Skyscan 1176; Skyscan; Aartselaar, Belgium). The analysis was performed using 50 kV, 800 μ A, 14.4 μ M resolution. After 3D reconstruction, the square ROI around the sagittal suture of the murine calvaria was selected as an analysis of further bone mass parameters. The detail information of this process protocol was based on our previous report (Wu et al., 2019). Structural parameters for the calvarias were measured with the built-in software using the bone volume/total volume (BV/TV), the number of porosity, and the percentage of total porosity as previously reported (Feng et al., 2018).

Statistical Analysis

Data was illustrated either as means \pm standard deviation (SD), or the representative one with all independent triplicates. Statistical analysis among or within groups was conducted by one-way ANOVA tests using SPSS 19.0 software (SPSS Inc., United States). * $p < 0.05$, ** $p < 0.01$, *** $p < 0.001$ was regarded as statistical significance.

RESULTS

CHR Suppressed RANKL-Induced Osteoclast Differentiation *In Vitro*

To investigate the effect of CHR (**Figure 1A**) on OC formation, murine BMMs were stimulated with RANKL and M-CSF in the absence or presence of CHR in dose- and time-dependent manners. As shown in **Figures 1B–E**, we found that various dose of CHR (5, 10, and 20 μ M) inhibited the number and size of TRAcP positive multinucleated OCs in a dose dependent way, wherein 20 μ M had the most pronounced effect. In order to examine the inhibition of CHR towards OC formation was in the time-dependent manner, murine BMMs stimulated with M-CSF and RANKL were exposed to CHR on day 1, 3, or 5. As with the dose-dependent effect, CHR also time-dependently inhibited the formation of mature TRAcP positive multinucleated OCs (**Figures 1F,G**) and significantly reduced the size of OC

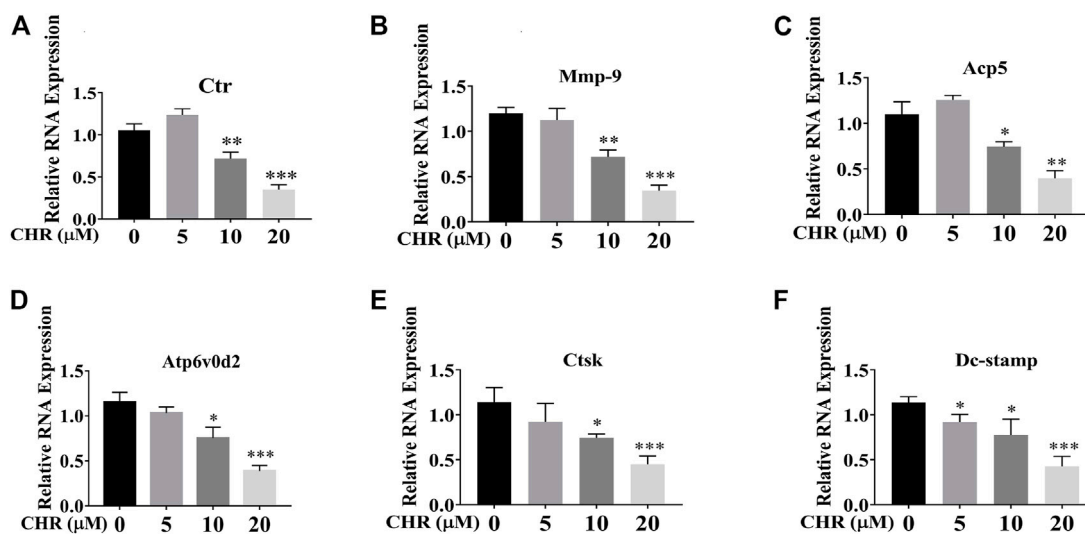


FIGURE 2 | CHR suppressed RANKL-induced expression of OC-associated genes. Murine BMMs were stimulated with 30 ng/ml M-CSF and 100 ng/ml RANKL in the absence or presence of indicated concentrations of CHR for 6 days to form multinucleated TRAcP positive OCs. Cells were lysed, RNA was extracted, and the cDNA generated from reverse transcription was subjected to real-time quantitative PCR using specific primers against OC-specific genes. **(A)** *Ctr*, **(B)** *Mmp-9*, **(C)** *Acp5*, **(D)** *Atp6v0d2*, **(E)** *Ctsk*, and **(F)** *Dc-Stamp*. Gene expression levels of *Ctr*, *Mmp9*, *Acp5*, *Atp6v0d2*, *Ctsk*, and *Dc-stamp* were expressed relative to control group ($n = 3$) (* $p < 0.05$, ** $p < 0.01$, *** $p < 0.001$).

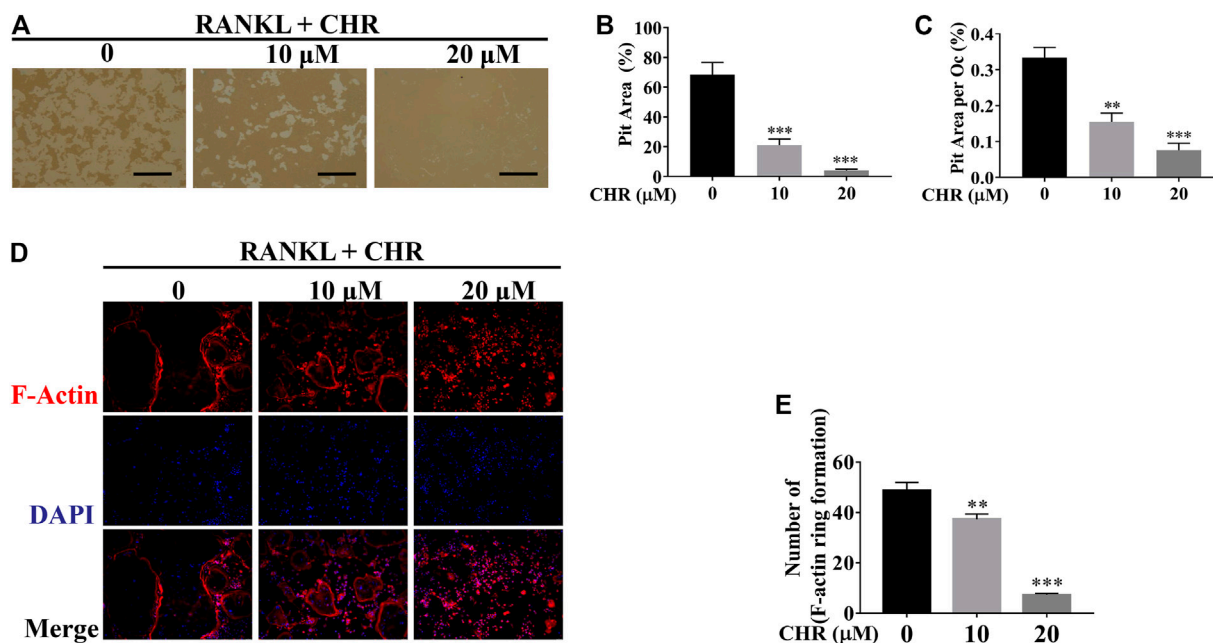


FIGURE 3 | CHR suppressed OC bone resorption and F-actin belts formation. **(A)** Mature OCs were seeded onto hydroxyapatite-coated plates and treated with indicated concentrations of CHR for 48 h. Attached cells were removed and micrographs of bone resorption pits (Magnification = $\times 100$; scale bar = 100 μm). **(B, C)** ImageJ was used to quantify the percentage of absorption pit area occupied by each osteoclast and the total absorption pit area. The data presented is a representative of three independent experiments and expressed as mean \pm SD. **(D)** CHR suppressed RANKL-induced F-actin belts formation. Murine BMM cells were stimulated with RANKL and M-CSF and treated with CHR (10 and 20 μM) as previously described. OCs formed were fixed and stained for F-actin and nuclei with Rhodamine-conjugated phalloidin and DAPI, respectively, and images captured using laser scanning confocal microscopy. The data presented is a representative of three independent experiments and expressed as mean \pm SD. **(E)** The numbers of OCs based on F-actin belts formation were quantified (** $p < 0.01$, *** $p < 0.001$ vs RANKL-treated controls.)

(Figures 1F,H) as compared with the untreated control. Treatment of CHR on day 1 or day 3 showed the most pronounced inhibitory effect (Figures 1F–H). To rule out the possibility of cytotoxicity, we performed CCK-8 viability assay on murine BMMs. As shown in Figure 1I, CHR demonstrated little to no cytotoxicity at concentrations up to 20 μ M. Collectively, these findings indicated that CHR inhibited OC formation through a mechanism that abrogates early RANKL-induced signaling cascades.

CHR Suppressed RANKL-Induced Osteoclast Gene Expression

We next assessed the suppression of CHR on RANKL-induced gene expression during OC formation. Expression levels of OC-related genes after 6-days stimulation of RANKL and M-CSF in the absence or presence of indicated concentrations of CHR were analyzed by real-time quantitative PCR. As shown in Figure 2, treatment with CHR dose-dependently suppressed the expression of genes related to OC formation and activity including *Ctr*, *Mmp9*, *Acp5*, *Atp6v0d2*, *Ctsk*, and *Dc-stamp* (Phan et al., 2004; Haotian et al., 2009).

CHR Inhibited Bone Resorption and F-Actin Formation

Next, we explored the effect of CHR on the bone resorptive activity of mature OCs. Equal number of mature OCs were seeded into hydroxyapatite coated plates and treated with 10 or 20 μ M of CHR for 48 h. Total resorbed areas were quantified by ImageJ. As shown in Figures 3A–C, percentage of average absorption area per osteoclast in CHR treated groups was significantly reduced as compared with positive controls. We next examined F-actin belts formation, a hallmark of actively resorbing OCs, using fluorescence microscopy. Mature OCs treated with indicated concentrations of CHR were stained for F-actin using Rhodamine-conjugated phalloidin and counterstained with DAPI to determine the number for nuclei per OC. As shown in Figures 3D,E, in the presence of CHR, the formation of F-actin rings were significantly reduced as compared with untreated controls, consistent with a reduction in size of the OC demonstrated in earlier experiments. Together, the results suggest that CHR can exert a suppression effect on RANKL-induced OC formation, fusion, and bone resorption in a dose-dependent manner.

CHR Inhibited RANKL-Induced NF- κ B and MAPK Signaling Pathways

The NF- κ B and MAPK signaling pathways play are critical for RANKL-induced OC formation (Ghosh and Karin, 2002). To determine the molecular mechanism by which CHR inhibits OC formation, we investigated the effects of CHR on the NF- κ B and MAPK signaling cascades. Murine BMMs were pretreated with or without 20 μ M of CHR and subsequently stimulated with 100 ng/ml RANKL for 5, 10, 20, 30, and 60 min. Total proteins were extracted from cells lysate and then subjected to Western blot. As

shown in Figures 4A–D RANKL-induced robust phosphorylation of ERK1/2, JNK1/2, p38 and I κ B α , reaching peak level of phosphorylation at around 10 min. On the other hand, in the presence of CHR, phosphorylated pERK1/2 and pJNK1/2, were significantly inhibited, whereas phosphorylated p38 remained unaffected.

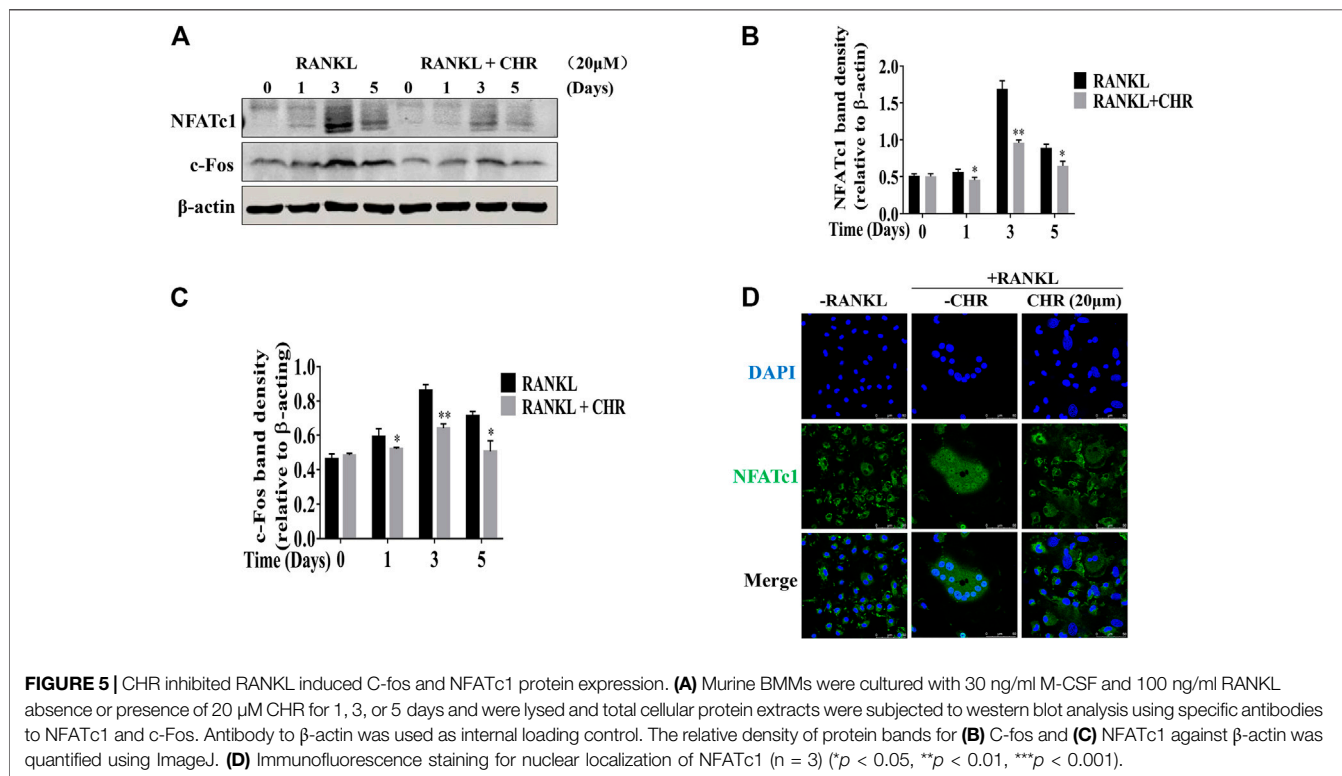
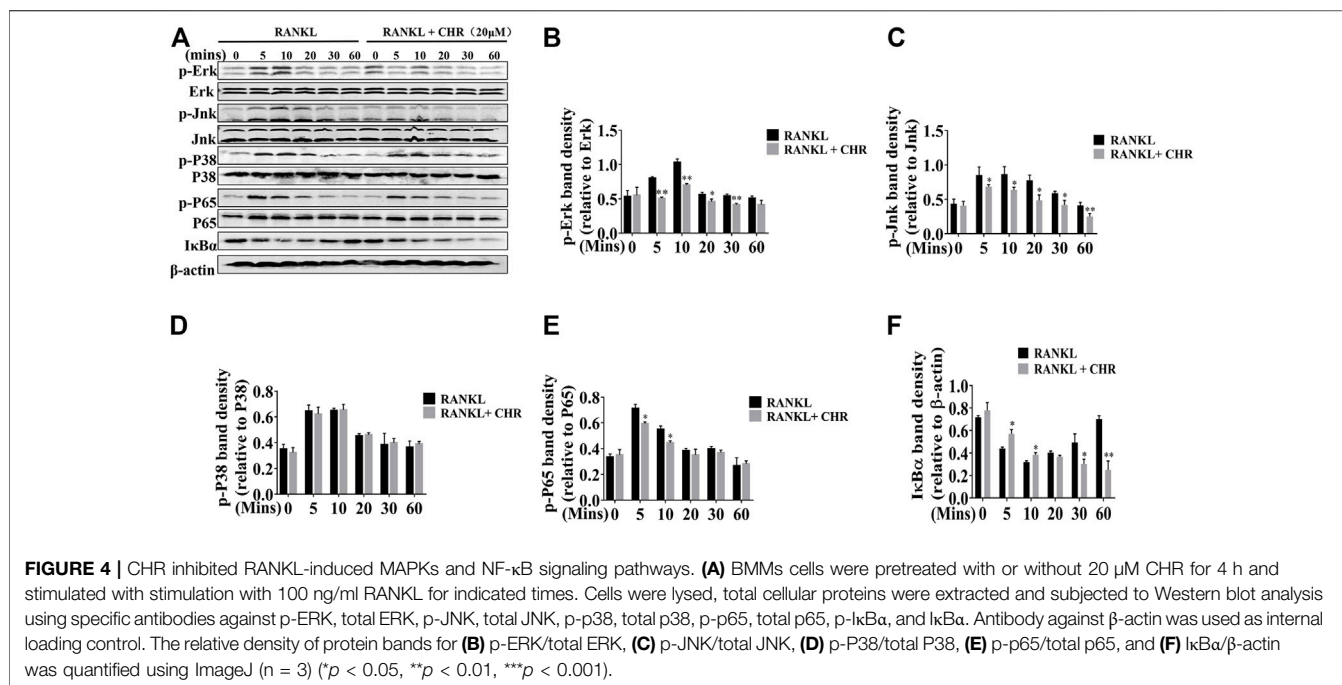
CHR similarly exerts inhibitory influence on RANKL-induced NF- κ B signaling. Rapid degradation of I κ B α is the hallmark for the activation of this signaling cascade. As shown in Figures 4A,E,F, I κ B α degraded within 5–10 min with RANKL stimulation, followed by a slow recovery towards basal levels from 20 to 60 min. The degradation of I κ B α proteins coincided with the phosphorylation of p65, which also reached peak level among 5 to 10 min after RANKL stimulation. In the presence of CHR, the phosphorylation of p65 was significantly reduced since the delayed degradation of I κ B α . Finally, the activation of NF- κ B and MAPK culminated the potency as the downstream activation of c-Fos and NFATc1. These two transcriptional factors were indispensable for OC formation and bone resorption (Ikeda et al., 2004; Monje et al., 2005). As can be seen from the results shown in Figures 5A–C, the expression of the RANKL-induced nuclear transcription factors c-Fos and NFATc1 in the nucleus was significantly reduced after treatment with CHR. In addition, as shown in Figure 5D our immunofluorescence assay demonstrated that NFATc1 nuclear translocation was inhibited after treatment with CHR.

Collectively, these results indicate that CHR inhibits both the NF- κ B and the MAPK pathways which subsequently down-regulates the expression of key OC transcription factors NFATc1 and c-Fos.

CHR Inhibited Titanium Particles-Induced Calvarial Osteolysis *In Vivo*

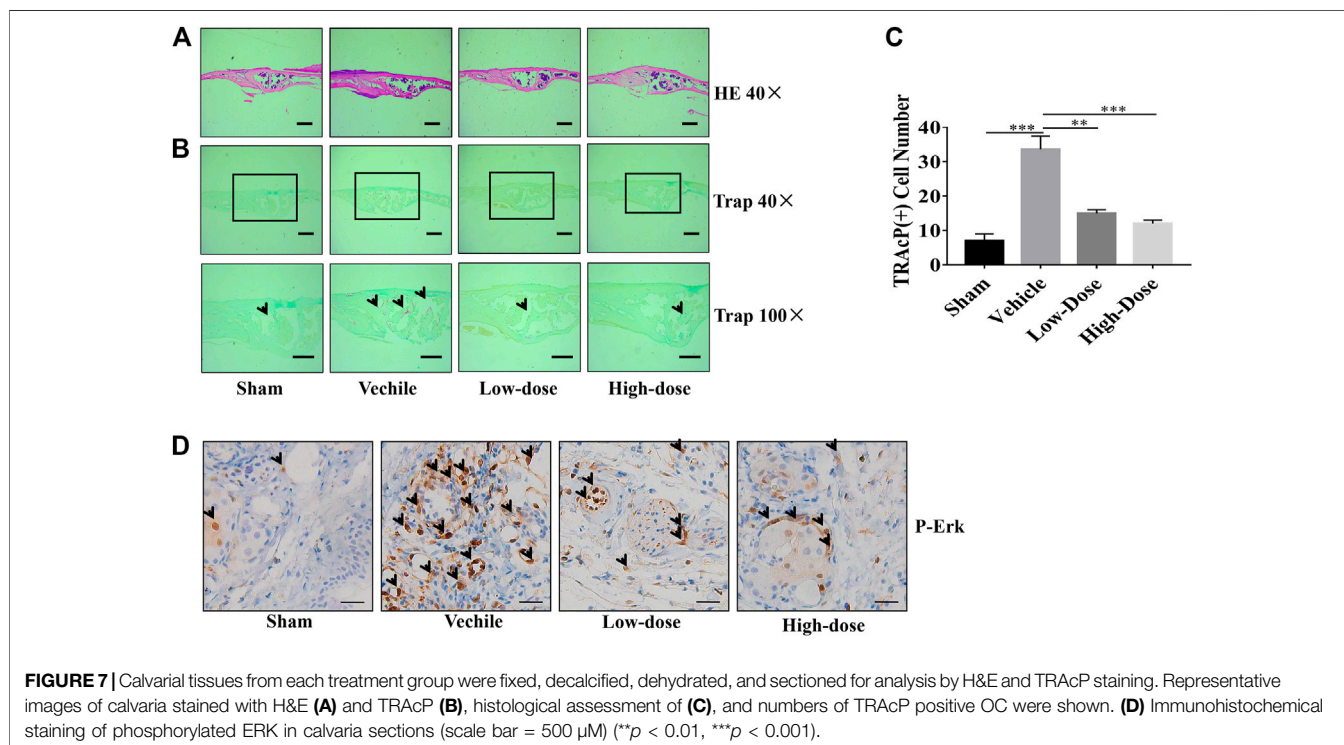
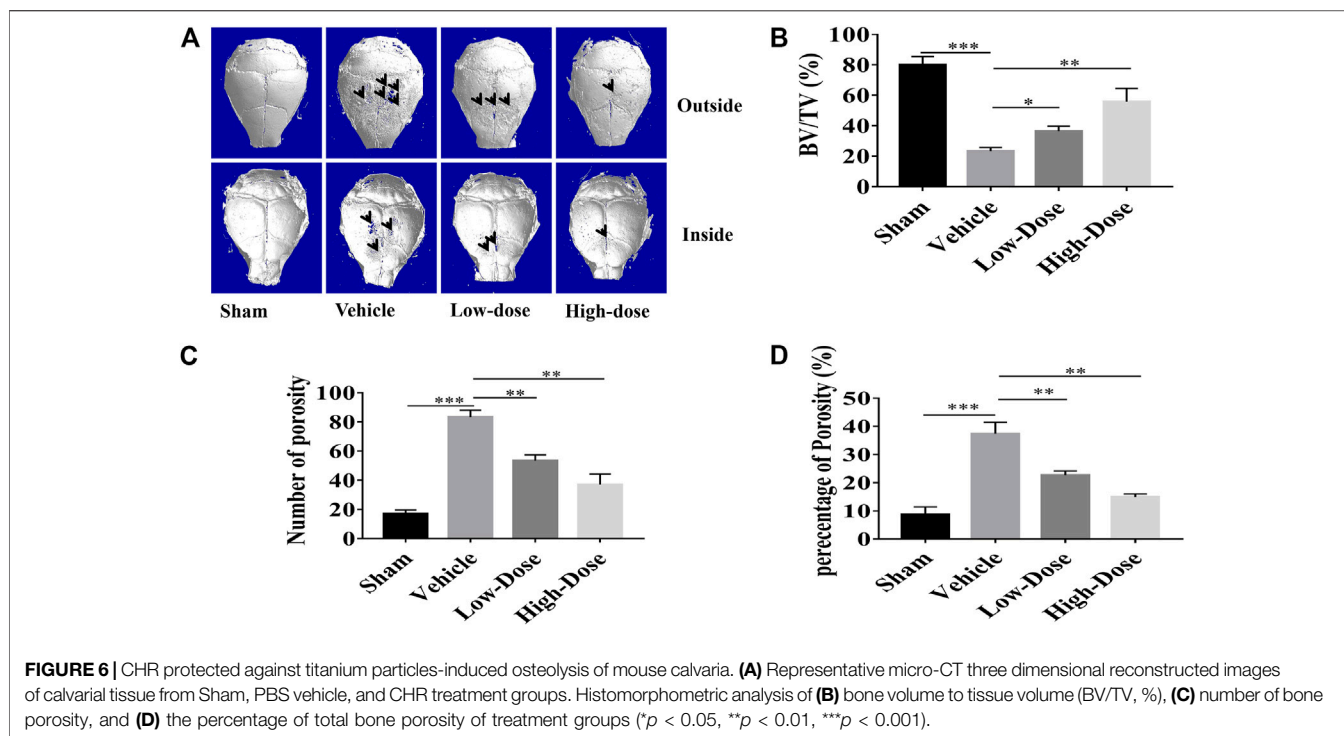
The titanium particles-induced calvarial osteolysis model was established to mimic *in vivo* function that CHR protected over-activation of osteoclast, as well as its predominant potential as being an anti-osteolytic agent. Thirty milligram titanium particles were implanted under the periosteum in all treating groups except the Sham group (no titanium particles). Mice in CHR-treated group were constantly injected for 2 weeks with 4 mg/kg (low dose) and 8 mg/kg (high dose); respectively every other day. Sham and vehicle groups were injected with the same volume of PBS every other day for 2 weeks. At the end of the experiment, titanium particles-induced calvarial bone destruction was examined using micro-CT scanning. Three dimensional reconstruction of the calvarial bone showed extensive bone resorption and destruction of the bone surface. On the other hand, the degree of surface bone resorption and destruction induced by titanium particles was dose-dependently alleviated in CHR-treated groups (Figure 6A).

Three major indicators of bone histomorphometric parameters, bone volume/tissue volume (BV/TV), the amount of bone porosity, and the percentage of total bone porosity, were applied for evaluation of bone integrity (Figures 6B–D). BV/TV of the calvarial bone was dose-



dependently increased following treatment with CHR as compared to the PBS-treated vehicle group (**Figure 6B**). Consistent with this effect, porosity number and the percentage of total porosity were also dose-dependently reduced towards Sham levels in CHR treated groups as

compared with PBS-treated vehicle group (**Figures 6C,D**). Histological images provided evidence that CHR protected calvarial osteolysis from titanium particles induction (**Figures 7A-C**). H&E and TRAcP staining showed serious bone destruction in the vehicle group with numerous TRAcP



positive multinucleated OCs and larger amounts of active OCs (Figures 7A–C) which accord to the micro-CT and histomorphometric results. Meanwhile, immunohistochemical staining showed significant activation of phosphorylated ERK in the vehicle group (Figure 7D), and the phosphorylated ERK in the

treatment group showed a downward trend, which was consistent with *in vitro* Western blot assay. Taken together, our *in vivo* data suggests that CHR has a protective effect against titanium particles-induced calvarial osteolysis via attenuation of OC formation and function as demonstrated in our *in vitro* experiments.

DISCUSSION

Over-activation of OCs in response to implant-derived wear particles remains the key cause of osteolysis around the prosthetic joints (Jiang et al., 2013; Langdahl et al., 2016). Clinically, drugs targeting OC formation and function have shown varying levels of effectiveness against osteolysis and osteoporosis. For example, although bisphosphonates have been clinically used for osteolytic conditions, their use is associated with a number of negative side effects including gastrointestinal complications, musculoskeletal pain, and osteonecrosis of the jaw (Verron and Bouler, 2014). Thus, there are still unmet needs for the discovery of novel agents that can specifically target the OC for the effective treatment of local osteolysis.

Traditional Chinese medicine monomers which extracted from natural plants such as Artesunate and Luteoloside have demonstrated inhibitory effect on OC formation and its biological function (Song et al., 2018; Wei et al., 2018). In the present study, for the first time we showed the protection ability of CHR in bone resorption of CHR *in vivo* and *in vitro*. This bioflavonoid was discovered with a good suppression of osteoclast formation, as well as delaying the bone resorption function of osteoclasts. Besides, *in vivo* verification illustrated bioactivity of CHR in preventing titanium particles-induced calvarial osteolysis after administration. Moreover, CHR demonstrated no cytotoxicity at a range of concentration (5–20 μ M) that inhibited OC formation and bone resorption through RANKL-induced pathways. Furthermore, our data also suggested that CHR exerted its inhibitory effect at early stage of OC formation. Consistent with the attenuation of RANKL-induced OC formation, the expression of OC marker genes such as *Ctr*, *Mmp9*, *Acp5*, *Atp6v0d2*, *Ctsk*, and *Dc-stamp* were down-regulated after treating with CHR. In addition, we found that CHR could inhibit F-actin belts formation in mature OCs.

The inhibitory effect of CHR on OC formation and function of bone resorption contributed to the protective effect of CHR on titanium particles-induced calvarial bone destruction mediated by OCs *in vivo*. Treatment with CHR every 2 days for 14 days effectively suppressed TRAcP positive OC formation and bone resorption induced by titanium particles. Micro-CT imaging and related histomorphometric analyses demonstrated the damage extent of calvarial bone was relieved in CHR treated groups. Histological assessment by H&E and TRAcP staining further verified that the reduction in bone loss was contributed to the drop of count of TRAcP positive OCs in CHR treated groups.

NF- κ B activation is one of the most significant early signaling events induced by RANKL, and perturbations in this signaling axis prevents osteoclastogenesis *in vitro* and leads to osteopetrosis *in vivo* (Soysa and Alles, 2009). On the other hand, over-activation of NF- κ B is associated with osteoclastic bone diseases (Xu et al., 2009). I κ B kinase (IKK) complex breaks the inactive statue of inhibitor- κ Bs (I κ Bs) by phosphorylation which essentially triggers the NF- κ B signaling activation. The rapid phosphorylation of I κ Bs and

its subsequent proteasome degradation permits the downstream phosphorylation, nuclear translocation, and activation of NF- κ B subunit p65/RelA (Iotsova et al., 1997). In our study, CHR markedly delayed I κ B α phosphorylation and degradation, and in turn suppressed nuclear translocation of p65/RelA.

Mitogen-activated protein kinase (MAPK) pathways include extracellular signal-regulated kinase (ERK), c-Jun n-terminal kinase (JNK), and p38, which are all rapidly phosphorylated in response to RANKL and also plays crucial roles in the early stages of OC formation, activation, and survival (Hotokezaka et al., 2002; Stevenson et al., 2011). In this study, we found that CHR could suppress the phosphorylation and activation of ERK and JNK, but not the activation of p38. CHR has also been shown to inhibit phosphorylation of ERK *in vivo*. The inhibition of ERK and JNK suggests that CHR may target a common upstream regulator (such as a common MEK) within the JNK/ERK axis, of which further investigations are required.

Following activation, the NF- κ B and MAPKs synergistically activate the transcriptional activities of key transcription factors in the nucleus c-Fos and NFATc1 (Miyamoto, 2011). In particular, NF- κ B is required for the initial induction of NFATc1 and the MAPK/c-Fos signaling axis plays an important role in further induction and activity of NFATc1. Being regarded as the prioritized and the most distal transcription factor, NFATc1 regulated OC-specific marker genes including *Ctr*, *Mmp9*, *Acp5*, *Atp6v0d2*, *Ctsk*, and *Dc-stamp* (Kim et al., 2008). Consistent with attenuated activation of ERK, JNK, and NF- κ B, the induction of c-Fos and NFATc1 proteins was significantly decreased in the presence of CHR. The reduced induction of NFATc1 protein expression suggests decrease transcriptional activity which was consistent with the observed decreased gene expression of *Ctr*, *Mmp9*, *Acp5*, *Atp6v0d2*, *Ctsk*, and *Dc-stamp* (Phan et al., 2004; Feng et al., 2009) in the presence of CHR. Our signaling experiments strongly suggest that the anti-osteoclastogenic effect of CHR can be attributed to inhibition of early NF- κ B and MAPK signaling pathway which in turns down-regulated the expression and activity of the master transcription regulator NFATc1 for OC formation.

Collectively, the results in our study demonstrated that CHR has a dramatic inhibition on osteoclastogenesis and function of bone resorption *in vitro* through the suppression of crucial RANKL-mediated signaling pathways. CHR exerted protective effects on titanium particles-induced osteolysis in the murine calvarial model *in vivo* by directly acting on OCs to attenuate OC-mediated bone destruction. These data presented in this study suggest that CHR is a potential therapeutic candidate for the attenuation of osteolytic diseases.

DATA AVAILABILITY STATEMENT

The original contributions presented in the study are included in the article/**Supplementary Material**, further inquiries can be directed to the corresponding authors.

ETHICS STATEMENT

The animal study was reviewed and approved by Animal Ethics Committee of Guangxi Medical University, Guangxi Medical University.

AUTHOR CONTRIBUTIONS

The authors acknowledged all the members of our laboratory for the help. ZW, CL, YC, QL, NL, XH, WL, RS, CW, FF, JD, SS, GY, LL, XS, DW, and YS carried out experiments, analyzed the data and prepared the figures; ZW wrote the main manuscript, JZ, JX, RX, XX, and FX designed the study and revised the manuscript. All authors reviewed the manuscript.

REFERENCES

- Arai, F., Miyamoto, T., Ohneda, O., Inada, T., Sudo, T., Brasel, K., et al. (1999). Commitment and Differentiation of Osteoclast Precursor Cells by the Sequential Expression of C-Fms and Receptor Activator of Nuclear Factor κ B (RANK) Receptors. *J. Exp. Med.* 190, 1741–1754. doi:10.1084/jem.190.12.1741
- Boyle, W. J., Simonet, W. S., and Lacey, D. L. (2003). Osteoclast Differentiation and Activation. *Nature* 423, 337–342. doi:10.1038/nature01658
- Feng, H., Cheng, T., Steer, J. H., Joyce, D. A., Pavlos, N. J., Leong, C., et al. (2009). Myocyte Enhancer Factor 2 and Microphthalmia-Associated Transcription Factor Cooperate with NFATc1 to Transactivate the V-ATPase D2 Promoter during RANKL-Induced Osteoclastogenesis. *J. Biol. Chem.* 284, 14667–14676. doi:10.1074/jbc.M901670200
- Feng, W., Li, J., Liao, S., Ma, S., Li, F., Zhong, C., et al. (2018). G66983 Attenuates Titanium Particle-Induced Osteolysis and RANKL Mediated Osteoclastogenesis through the Suppression of NF κ B/JNK/p38 Pathways. *Biochem. Biophysical Res. Commun.*, S0006291X18312543. doi:10.1016/j.bbrc.2018.05.177
- Funakoshi-Tago, M., Ohsawa, K., Ishikawa, T., Nakamura, F., Ueda, F., Narukawa, Y., et al. (2016). Inhibitory Effects of Flavonoids Extracted from Nepalese Propolis on the LPS Signaling Pathway. *Int. Immunopharmacol.* 40, 550–560. doi:10.1016/j.intimp.2016.10.008
- Ghosh, S., and Karin, M. (2002). Missing Pieces in the NF- κ B Puzzle. *Cell* 109 Suppl, S81–S96. doi:10.1016/s0092-8674(02)00703-1
- Ha, S. K., Moon, E., and Kim, S. Y. (2010). Chrysin Suppresses LPS-Stimulated Proinflammatory Responses by Blocking NF- κ B and JNK Activations in Microglia Cells. *Neurosci. Lett.* 485, 143–147. doi:10.1016/j.neulet.2010.08.064
- Hadjidakis, D. J., and Androulakis, I. I. (2006). Bone Remodeling. *Ann. N. Y. Acad. Sci.* 1092, 385–396. doi:10.1196/annals.1365.035
- Hotokezaka, H., Sakai, E., Kanaoka, K., Saito, K., Matsuo, K., Kitaura, H., et al. (2002). U0126 and PD98059, Specific Inhibitors of MEK, Accelerate Differentiation of RAW264.7 Cells into Osteoclast-like Cells. *J. Biol. Chem.* 277, 47366–47372. doi:10.1074/jbc.M208284200
- Ikeda, F., Nishimura, R., Matsubara, T., Tanaka, S., Inoue, J., Reddy, S. V., et al. (2004). Critical Roles of C-Jun Signaling in Regulation of NFAT Family and RANKL-Regulated Osteoclast Differentiation. *J. Clin. Invest.* 114, 475–484. doi:10.1172/JCI19657
- Iotsova, V., Caamaño, J., Loy, J., Yang, Y., Lewin, A., and Bravo, R. (1997). Osteopetrosis in Mice Lacking NF- κ B1 and NF- κ B2. *Nat. Med.* 3, 1285–1289. doi:10.1038/nm1197-1285
- Jiang, Y., Jia, T., Gong, W., Wooley, P. H., and Yang, S. Y. (2013). Titanium Particle-Challenged Osteoblasts Promote Osteoclastogenesis and Osteolysis in a Murine Model of Periprosthetic Osteolysis. *Acta Biomater.* 9, 7564–7572. doi:10.1016/j.actbio.2013.03.010
- Kim, J., Yang, J., Park, O. J., Kang, S. S., Kim, W. S., Kurokawa, K., et al. (2013). Lipoproteins Are an Important Bacterial Component Responsible for Bone

FUNDING

This work was supported in part by Program of China (2020YFA0112900) and National Natural Science Foundation of China (81972034, 92068104 to RX), Guangxi Natural Science Foundation Award (2018GXNSFAA294053 to JZ), Natural Science Foundation of Fujian Province (2020J05008 to YC).

SUPPLEMENTARY MATERIAL

The Supplementary Material for this article can be found online at: <https://www.frontiersin.org/articles/10.3389/fphar.2022.793087/full#supplementary-material>

- Destruction through the Induction of Osteoclast Differentiation and Activation. *J. Bone Miner Res.* 28, 2381–2391. doi:10.1002/jbmr.1973
- Kim, K., Lee, S. H., Ha Kim, J., Choi, Y., and Kim, N. (2008). NFATc1 Induces Osteoclast Fusion via Up-Regulation of Atp6v0d2 and the Dendritic Cell-specific Transmembrane Protein (DC-STAMP). *Mol. Endocrinol.* 22, 176–185. doi:10.1210/me.2007-0237
- Kular, J., Tickner, J., Chim, S. M., and Xu, J. (2012). An Overview of the Regulation of Bone Remodelling at the Cellular Level. *Clin. Biochem.* 45, 863–873. doi:10.1016/j.clinbiochem.2012.03.021
- Lacey, D. L., Timms, E., Tan, H. L., Kelley, M. J., Dunstan, C. R., Burgess, T., et al. (1998). Osteoprotegerin Ligand Is a Cytokine that Regulates Osteoclast Differentiation and Activation. *Cell* 93, 165–176. doi:10.1016/s0092-8674(00)81569-x
- Langdahl, B., Ferrari, S., and Dempster, D. W. (2016). Bone Modeling and Remodeling: Potential as Therapeutic Targets for the Treatment of Osteoporosis. *Ther. Adv. Musculoskelet. Dis.* 8, 225–235. doi:10.1177/1759720X16670154
- Masanori, K., Saya, K., Tadashi, N., Toshihide, M., Teruhito, Y., Kazuhiro, M., et al. (2010). Diphenylhydantoin Inhibits Osteoclast Differentiation and Function through Suppression of NFATc1 Signaling. *J. Bone Mineral Res.* 24, 1469–1480.
- Matsuo, K., Galson, D. L., Zhao, C., Peng, L., Laplace, C., Wang, K. Z., et al. (2004). Nuclear Factor of Activated T-Cells (NFAT) Rescues Osteoclastogenesis in Precursors Lacking C-Fos. *J. Biol. Chem.* 279, 26475–26480. doi:10.1074/jbc.M313973200
- Miyamoto, T. (2011). Regulators of Osteoclast Differentiation and Cell-Cell Fusion. *Keio J. Med.* 60, 101–105. doi:10.2302/kjm.60.101
- Monje, P., Hernández-Losa, J., Lyons, R. J., Castellone, M. D., and Gutkind, J. S. (2005). Regulation of the Transcriptional Activity of C-Fos by ERK. A Novel Role for the Prolyl Isomerase PIN1. *J. Biol. Chem.* 280, 35081–35084. doi:10.1074/jbc.C500353200
- Nagasaka, M., Hashimoto, R., Inoue, Y., Ishiuchi, K., Matsuno, M., Itoh, Y., et al. (2018). Anti-Tumorigenic Activity of Chrysin from *Oroxylum Indicum* via Non-genotoxic P53 Activation through the ATM-Chk2 Pathway. *Molecules* 23, 1394. doi:10.3390/molecules23061394
- Nakashima, T., and Takayanagi, H. (2015). New Regulation Mechanisms of Osteoclast Differentiation. *Ann. N. Y. Acad. Sci.* 1240, E13–E18. doi:10.1111/j.1749-6632.2011.06373.x
- Nile, S. H., Keum, Y. S., Nile, A. S., Jalde, S. S., and Patel, R. V. (2017). Antioxidant, Anti-inflammatory, and Enzyme Inhibitory Activity of Natural Plant Flavonoids and Their Synthesized Derivatives. *J. Biochem. Mol. Toxicol.* 32. doi:10.1002/jbt.22002
- Norman, P. (2002). Natural Products as a Source of New Drugs. *Drug News Perspect.* 15, 461
- Phan, T. C., Xu, J., and Zheng, M. H. (2004). Interaction between Osteoblast and Osteoclast: Impact in Bone Disease. *Histol. Histopathol.* 19, 1325–1344. doi:10.14670/HH-19.1325
- Qin, A., Cheng, T. S., Lin, Z., Cao, L., Chim, S. M., Pavlos, N. J., et al. (2012). Prevention of Wear Particle-Induced Osteolysis by a Novel V-ATPase Inhibitor Saliphenylhalamide through Inhibition of Osteoclast Bone Resorption. *Plos One* 7, e34132. doi:10.1371/journal.pone.0034132

- Song, F., Wei, C., Zhou, L., Qin, A., Yang, M., Tickner, J., et al. (2018). Luteoloside Prevents Lipopolysaccharide-Induced Osteolysis and Suppresses RANKL-Induced Osteoclastogenesis through Attenuating RANKL Signaling Cascades. *J. Cel. Physiol.* 233, 1723–1735. doi:10.1002/jcp.26084
- Soysa, N. S., and Alles, N. (2009). NF-kappaB Functions in Osteoclasts. *Biochem. Biophys. Res. Commun.* 378, 1–5. doi:10.1016/j.bbrc.2008.10.146
- Stevenson, D. A., Schwarz, E. L., Carey, J. C., Viskochil, D. H., Hanson, H., Bauer, S., et al. (2011). Bone Resorption in Syndromes of the Ras/MAPK Pathway. *Clin. Genet.* 80, 566–573. doi:10.1111/j.1399-0004.2010.01619.x
- Teitelbaum, S. L. (2000). Bone Resorption by Osteoclasts. *Science* 289, 1504–1508. doi:10.1126/science.289.5484.1504
- Thaler, R., Maurizi, A., Roschger, P., Sturmlechner, I., Khani, F., Spitzer, S., et al. (2016). Anabolic and Antiresorptive Modulation of Bone Homeostasis by the Epigenetic Modulator Sulforaphane, a Naturally Occurring Isothiocyanate. *J. Biol. Chem.* 291, 6754–6771. doi:10.1074/jbc.M115.678235
- Verron, E., and Boulter, J. M. (2014). Is Bisphosphonate Therapy Compromised by the Emergence of Adverse Bone Disorders. *Drug Discov. Today* 19, 312–319. doi:10.1016/j.drudis.2013.08.010
- Wang, J., Wang, H., Sun, K., Wang, X., Pan, H., Zhu, J., et al. (2018). Chrysin Suppresses Proliferation, Migration, and Invasion in Glioblastoma Cell Lines via Mediating the ERK/Nrf2 Signaling Pathway. *Drug Des. Devel. Ther.* 12, 721–733. doi:10.2147/DDDT.S160020
- Wang, T., Liu, Q., Tjohio, W., Zhao, J., Lu, A., Zhang, G., et al. (2017). Therapeutic Potential and Outlook of Alternative Medicine for Osteoporosis. *Curr. Drug Targets* 18, 1051–1068. doi:10.2174/1389450118666170321105425
- Wei, C. M., Liu, Q., Song, F. M., Lin, X. X., Su, Y. J., Xu, J., et al. (2018). Artesunate Inhibits RANKL-Induced Osteoclastogenesis and Bone Resorption *In Vitro* and Prevents LPS-Induced Bone Loss *In Vivo*. *J. Cel Physiol* 233, 476–485. doi:10.1002/jcp.25907
- Wooley, P. H., and Schwarz, E. M. (2004). Aseptic Loosening. *Gene Ther.* 11, 402–407. doi:10.1038/sj.gt.3302202
- Wu, J., Guan, R., Cao, G., Liu, Z., Wang, Z., Shen, H., et al. (2018). Antioxidant and Antimicrobial Effects of Catechin Liposomes on Chinese Dried Pork. *J. Food Prot.* 81, 827–834. doi:10.4315/0362-028X.JFP-17-452
- Wu, Z., Wu, H., Li, C., Fu, F., Ding, J., Shao, S., et al. (2019). Daphnetin Attenuates LPS-Induced Osteolysis and RANKL Mediated Osteoclastogenesis through Suppression of ERK and NFATc1 Pathways. *J. Cell Physiol.* 234 (10), 17812–17823. doi:10.1002/jcp.28408
- Xu, J., Tan, J. W., Huang, L., Gao, X. H., Laird, R., Liu, D., et al. (2000). Cloning, Sequencing, and Functional Characterization of the Rat Homologue of Receptor Activator of NF-kappaB Ligand. *J. Bone Miner Res.* 15, 2178–2186. doi:10.1359/jbmr.2000.15.11.2178
- Xu, J., Wu, H. F., AngYip, E. S., Yip, K., Woloszyn, M., Zheng, M. H., et al. (2009). NF-kappaB Modulators in Osteolytic Bone Diseases. *Cytokine Growth Factor Rev.* 20, 7–17. doi:10.1016/j.cytogfr.2008.11.007
- Yunpeng, J., Tanghong, J., Wooley, P. H., and Shang-You, Y. (2013). Current Research in the Pathogenesis of Aseptic Implant Loosening Associated with Particulate Wear Debris. *Acta Orthopaedica Belgica* 79, 1–9. PMID: 23547507.
- Zeinali, M., Meybodi, N. T., Rezaee, S. A., Rafatpanah, H., and Hosseinzadeh, H. (2017). Protective Effects of Chrysin on Sub-acute Diazinon-Induced Biochemical, Hematological, Histopathological Alterations, and Genotoxicity Indices in Male BALB/c Mice. *Drug Chem. Toxicol.* 1, 834. doi:10.1080/01480545.2017.1384834
- Zhang, L., Feng, M., Li, Z., Zhu, M., Fan, Y., Chu, B., et al. (2018). Bulleyaconitine A Prevents Ti Particle-Induced Osteolysis via Suppressing NF-Kb Signal Pathway during Osteoclastogenesis and Osteoblastogenesis. *J. Cel. Physiol.* 233, 7067–7079. doi:10.1002/jcp.26508

Conflict of Interest: The authors declare that the research was conducted in the absence of any commercial or financial relationships that could be construed as a potential conflict of interest.

Publisher's Note: All claims expressed in this article are solely those of the authors and do not necessarily represent those of their affiliated organizations, or those of the publisher, the editors, and the reviewers. Any product that may be evaluated in this article, or claim that may be made by its manufacturer, is not guaranteed or endorsed by the publisher.

Copyright © 2022 Wu, Li, Chen, Liu, Li, He, Li, Shen, Li, Wei, Shao, Fu, Ding, Sun, Wang, Yuan, Su, Zhao, Xu, Xu, Xu and Xu. This is an open-access article distributed under the terms of the Creative Commons Attribution License (CC BY). The use, distribution or reproduction in other forums is permitted, provided the original author(s) and the copyright owner(s) are credited and that the original publication in this journal is cited, in accordance with accepted academic practice. No use, distribution or reproduction is permitted which does not comply with these terms.